

Examining the Thermal Stability of an Al-Mg-Sc alloy processed by High-Pressure Torsion

Pedro Henrique R. Pereira ^{a,b,*}, Yi Huang ^a and Terence G. Langdon ^a

^aMaterials Research Group, Faculty of Engineering and the Environment
University of Southampton, Southampton SO17 1BJ, U.K.

^bCAPES Foundation, Ministry of Education of Brazil, Brasília - DF 70040-020, Brazil.

Abstract

An Al-3%Mg-0.2%Sc alloy was solution treated and subjected to 10 turns of high-pressure torsion (HPT). Thereafter, the HPT-processed material was annealed for 1 hour at temperatures ranging from 423 to 773 K and its mechanical properties and microstructural evolution were examined using microhardness measurements and EBSD analysis. The results demonstrate that the Al-Mg-Sc alloy exhibits an average microhardness of ~190 Hv and an average grain size of ~140 nm immediately after HPT processing and also after further annealing at 423 K. Conversely, it is shown that annealing at temperatures above 473 K leads to a substantial decrease in the hardness values as well as a sharp increase in the grain size of the material previously processed by HPT. In addition, detailed EBSD analysis revealed the formation of a bi-modal distribution of grains after annealing at temperatures from 623 to 773 K, and this becomes more uniform with increasing temperatures.

Keywords: Aluminium alloys, Hall-Petch relationship, Hardness, High-pressure torsion, Severe plastic deformation, Thermal stability.

*Corresponding author: Pedro Henrique R. Pereira (email: phrp1d13@soton.ac.uk)

1. Introduction

The growing interest for more fuel-efficient vehicles has motivated the development of Al alloys with high strength to density ratio, especially designed for applications in the automotive and aerospace industries^{1,2}. Severe plastic deformation (SPD)^{3,4} techniques have been successfully used to produce ultrafine-grained (UFG) Al alloys with significantly enhanced mechanical strength and superplastic properties by comparison with metals subjected to conventional metal forming⁵. Among the various SPD methods, major attention has been devoted to equal-channel angular pressing (ECAP)⁶, and especially to high-pressure torsion (HPT)⁷ as this procedure is more effective in fabricating UFG metals with grain sizes in the nanometre range ($<0.1 \mu\text{m}$).

Al-Mg alloys processed by ECAP⁸⁻¹⁰ and HPT^{11,12} display superior mechanical strength compared with the coarse-grained material as a consequence of the intense strain hardening and grain refinement introduced during severe plastic deformation. The UFG Al-3Mg alloy has an average grain size of $\sim 0.27 \mu\text{m}$ and a yield stress of $\sim 400 \text{ MPa}$ after processing by 8 passes of ECAP at room temperature using route B_c⁸. In addition, even finer grain structures and further strengthening may be obtained after HPT processing, as recently reported for different Al-Mg alloys with % Mg in weight of ≥ 1 ^{11,12}. However, Al-Mg alloys usually exhibit early recrystallization and abnormal grain growth after SPD processing and subsequent heat treatment at relatively low temperatures¹¹⁻¹⁴, thereby limiting their applications as structural components. Therefore, with the aim of improving the thermal stability of Al-Mg alloys, these metals may be alloyed with Sc additions because Al₃Sc precipitates are effective in pinning the grain boundaries and retaining ultrafine grains even at high temperatures¹⁵⁻¹⁸.

Several investigations have demonstrated the outstanding mechanical properties and superplastic behaviour of Al-Mg-Sc alloys processed by ECAP¹⁹⁻²². Elongations of $> 2000 \%$ ^{19,20} were attained in the ECAP-processed material tested in tension at $T \geq 673 \text{ K}$ at initial

strain rates, $\dot{\epsilon}$, higher than $1.0 \times 10^{-2} \text{ s}^{-1}$. Furthermore, it is interesting to note that even after annealing at 723 K for 1 h, Al-Mg-Sc alloys processed by ECAP at different temperatures remain with grain structures with an average size of $<3 \mu\text{m}^{15,18}$.

There are numerous studies showing that processing Al-Mg-Sc alloys by HPT leads to additional grain refinement and improved strength by comparison with the ECAP-processed metal²³⁻²⁷. Conversely, it was revealed in a recent investigation²⁸ that, although excellent low temperature superplasticity is achieved in the Al-3Mg-0.2Sc alloy processed by 10 turns of HPT, the elongations to failure after tensile testing at $T \geq 623 \text{ K}$ are notable inferior by comparing with the material processed by ECAP. Therefore, more information is needed to fully assess the microstructural evolution of the HPT-processed alloy when exposed to elevated temperatures. Accordingly, the present study aims to evaluate the thermal stability of the Al-3Mg-0.2Sc alloy subjected to 10 turns of HPT processing by examining the mechanical properties and microstructural changes in this UFG alloy after annealing at temperatures up to 773 K for 1 h.

2. Experimental material and procedures

An Al-3% Mg-0.2% Sc (in wt. %) alloy was supplied by China Rare Metal Material Corporation (Jiangxi Province, China) in the form of forged rods with 130 mm length and a diameter of 10 mm. These rods were solution treated at $880 \pm 2 \text{ K}$ for 1 h and then quenched in water. Discs with a thickness of $\sim 1 \text{ mm}$ were cut from the heat treated metal and then were ground to a final thickness of $\sim 0.8 \text{ mm}$.

Afterwards, the Al alloy was subjected to 10 turns of quasi-constrained HPT processing²⁹⁻³⁰ at an initial temperature of $\sim 300 \text{ K}$. Initially, in the compression stage of HPT processing³¹, the discs were placed in a shallow central depression in the lower anvil and an axial load was applied at the surface of the samples in order to provide a nominal pressure of 6.0 GPa. The axial load was maintained constant and the lower anvil was rotated for 10 turns at a constant rate of 1 rpm imposing high torsional straining within the material.

Following HPT processing, discs were annealed at temperatures from 423 to 773 K for 1 h and cooled in air. Thereafter, both the HPT-processed material and the annealed samples were ground and polished to a mirror like quality and hardness measurements were taken at the middle-section of the discs following the same procedure described in earlier studies^{27,32}. The values of the Vickers microhardness were recorded using an FM300 microhardness tester equipped with a Vickers indenter under a load of 200 gf and a dwell time of 15 s. Hardness values were evaluated along the diameters of the discs at positions separated by 0.3 mm such that the microhardness in each position was calculated as the average of the measurements taken from four indentations separated by a distance of 0.15 mm. In addition, the area-weighted average microhardness of the Al-3Mg-0.2Sc alloy was estimated using the hardness values recorded along the diameter of the discs as the measurements taken at increasing distance from the centre of the disc are associated with larger surface areas.

The microstructure of the HPT-processed material was examined by scanning electron microscopy (SEM) and orientation imaging microscopy (OIM) through electron backscattered diffraction (EBSD). Samples were ground, polished using 1 μm diamond paste and 0.06 μm silica colloidal and then etched using an aqueous solution of 5 % HBF_4 .

The grain structures of the Al-Mg-Sc alloy were observed using a JSM6500F thermal field emission SEM and the average grain size, d , was estimated using the linear intercept method. EBSD patterns with information about the local crystal orientation were collected on a regular grid using step sizes as small as 0.07 μm and these were ultimately used to generate orientation maps for the HPT-processed metal annealed at $T \geq 573$ K. A cleaning procedure, including grain dilatation, was performed on each of these maps, henceforth denoted OIM images, such that the total number of modified points was <20 % for all points measured. Low-angle grain boundaries (LAGBs) were defined as having misorientation differences between adjacent points from 2° to 15° and high-angle grain boundaries (HAGBs) had

misorientations $>15^\circ$. The grain structures with HAGBs were coloured as a function of the grain sizes in each OIM image using a rainbow spectrum.

3. Experimental results

The variation of Vickers microhardness along the diameter of the Al-Mg-Sc discs processed by HPT and further annealed is depicted in Figure 1, where the hardness measurements of the HPT-processed sample are denoted by open circles. The solution treated material exhibits a uniform microhardness distribution with hardness values of ~ 58 Hv. Nevertheless, it is clearly seen that processing through 10 turns of HPT at ambient temperature leads to an intense hardening in this Al alloy, especially in the outer periphery of the disc in which hardness values >200 Hv were detected as in earlier investigations²⁷. In addition, it is apparent that the microhardness distribution remains inhomogeneous after HPT processing and lower hardness values (~ 120 Hv) are observed in the centre of the disc.

It is readily noted from Figure 1 that after annealing at 473 K there is a substantial decrease in the microhardness of the HPT-processed material and the hardness distribution becomes fairly homogeneous, except at the central region of the sample wherein the hardness measurements are similar to those observed immediately after HPT processing. Additionally, annealing at $T \geq 573$ K results in a further reduction of the Vickers microhardness as well as a more uniform microhardness distribution in the HPT-processed discs. Conversely, local hardness variations of the order of ~ 10 Hv are evident in the middle-section of the Al alloy annealed at 623 K for 1 h.

In order provide information about the softening kinetics in Al-Mg-Sc alloys exposed to elevated temperatures, Figure 2 shows the variation of the area-weighted average microhardness with the annealing temperature for Al-3Mg-0.2Sc discs processed by HPT and further annealed for 1 h. The results reveal that the Al alloy exhibits an average microhardness of ~ 190 Hv after 10 turns of HPT and subsequent annealing at $T \leq 423$ K.

However, the results show that annealing at the temperature range from 473 to 623 K leads to a substantial reduction in the hardness values of the material previously processed by HPT. In addition, it is also apparent in Figure 2 that the Vickers microhardness continues to decrease but at a lower rate after annealing at $T \geq 673$ K.

The grain boundaries of the Al-3Mg-0.2Sc alloy become evident after etching using an aqueous solution of 5% HBF₄. Accordingly, SEM images were obtained for the material processed by HPT as well as for the annealed discs and these images were used to estimate the grain size in each experimental condition with the aim of visualizing the variation of the grain size as a function of the annealing temperature for this Al alloy as shown in Figure 3.

The microstructure of the unprocessed Al-Mg-Sc alloy was fairly homogeneous and had an average grain size of $\sim 300 \mu\text{m}$ ²⁷. Processing through 10 turns of HPT produced significant grain refinement in this Al alloy such that $d \approx 0.14 \mu\text{m}$ as measured using SEM images taken at ~ 3 mm from the centre of the disc. This refinement is consistent with other reports that used TEM images for estimating the grain size after HPT processing²³⁻²⁵. As depicted in Figure 3, there is no relevant increase in the size of the grain structures after annealing at $T \leq 473$ K. However, the grain sizes grow rapidly for $T \geq 523$ K such that $d > 1 \mu\text{m}$ after annealing at 623 K and the average grain size is $\sim 6.2 \mu\text{m}$ for the material heat treated at 773 K for 1 h.

Figure 4 shows typical OIM images of the Al-3Mg-0.2Sc alloy processed by HPT at 300 K and further annealed at (a) 573, (b) 623 and (c) 773 K. In addition, the grains were coloured using a rainbow spectrum such that small structures with HAGBs are blue and larger grains have shades of red. It is readily apparent from Figure 4 (a) that the UFG material annealed at 573 K has a uniform distribution of submicrometre grains with an average size of $\sim 0.5 \mu\text{m}$ even after heat treatment for 1 h. Furthermore, substructures with LAGBs are seldom observed within the grains with HAGBs.

Conversely, inspection of Figure 4 (b) reveals that there is an abnormal grain growth in the microstructure of the Al alloy annealed at 623 K. The grain size in the grains coloured in blue is $\sim 1 \mu\text{m}$ whereas more than 70 % of the area fraction of the analysed image corresponds to large grains with $d > 10 \mu\text{m}$ containing a notable fraction of LAGBs in their interior. After annealing at $T > 673 \text{ K}$, the fraction of coarse grains further increases as well as the grain sizes and the microstructural homogeneity and subgrains are clearly seen in Figure 4 (c) for the HPT-processed material annealed at 773 K.

4. Discussion

The plots depicted in Figures 2 and 3 reveal that HPT processing leads to a significant hardening and grain refinement in Al-Mg alloys with Sc additions such that the Al-3Mg-0.2Sc alloy exhibits hardness values of $\sim 200 \text{ Hv}$ and an average grain size of $\sim 0.14 \mu\text{m}$ after 10 turns of HPT at 300 K. Nevertheless, the grain structures of this material become unstable and there is major grain coarsening after 1 h annealing at $T > 573 \text{ K}$.

The microhardness distribution is reasonably uniform along the diameter of the HPT-processed metal after annealing at 573 K for 1 h. Accordingly, Figure 4 (a) shows that a homogeneous microstructure develops in this material at the same annealing conditions. However, it is apparent in Figures 4 (b) and (c) that there is abnormal grain growth in the UFG alloy after annealing at $T \geq 623 \text{ K}$ as noted by its bi-modal grain distribution which also confirms the local hardness fluctuations observed in Figure 1.

An early investigation on the precipitation kinetics of a solution treated Al-0.2%Sc alloy³³ revealed that the nano-sized Al_3Sc precipitates are uniformly distributed within the microstructure of the Al-Sc alloy after heat treatment at temperatures below 623 K, whereas aging at $T \geq 643 \text{ K}$ leads to an inhomogeneous distribution of dispersoids which start precipitating after aging times of the order of a few minutes. In the current study, discontinuous grain growth is clearly evident in the HPT-processed Al-3Mg-0.2Sc alloy after annealing for 1 h at 623 and 673 K. Accordingly, as these temperatures are equivalent to the

transition temperature between continuous and discontinuous precipitation of Al_3Sc dispersoids in Al-Sc alloys, it is readily apparent that the formation of a bi-modal grain structure in the Al-3Mg-0.2Sc alloy is directly associated to the occurrence of discontinuous precipitation in the HPT-processed material during annealing. Furthermore, the continuous precipitation of Al_3Sc dispersoids at $T \leq 573$ K inhibits the occurrence of abnormal grain growth at low homologous temperatures as observed for pure nickel after processing by 10 turns of HPT at 300 K and further annealing at 448 K³⁴.

The formation of a duplex structure in UFG materials after annealing was also reported for an Al-3Mg alloy processed by ECAP¹⁴ and ECAP + cold rolling¹³. Nevertheless, recrystallization starts at lower temperatures (~ 500 K) by comparison with the Al-3Mg-0.2Sc alloy processed by HPT at room temperature. The Al-3Mg alloy has an average grain size of ~ 0.25 μm after 8 passes of ECAP using a die with a channel angle of $\sim 120^\circ$. Following annealing at 523 K for 1 h, the same material depicts a bi-modal grain distribution composed of fine grains with an average size of ~ 0.35 μm and coarse structures with $d \approx 5$ μm ¹⁴. Therefore, the exceptional effectiveness of the Al_3Sc dispersoids on delaying recrystallization in Al-Mg alloys is confirmed in this investigation, as the Al-3Mg-0.2Sc alloy processed by HPT exhibits smaller average grain sizes after annealing at identical conditions and there is no evidence of abnormal grain growth for $T < 623$ K.

It is interesting to note that the Al-3Mg alloy processed by ECAP + rolling is fully recrystallized after annealing at $T \geq 563$ K¹³, however the structures with HAGBs continue growing with increasing annealing temperatures and their average sizes exceed 20 μm after annealing at $T > 600$ K. By contrast, the HPT-processed Al-Mg-Sc alloy has an average grain size of ~ 6.2 μm even after annealing at 773 K and there are few remaining fine structures as apparent in Figure 4 (c).

The mechanical properties and microstructural evolution of Al-Mg alloys processed by HPT was examined in detail in recent reports^{11,12}. It was revealed that the hardness in the Al-1Mg alloy saturates at ~110 Hv already after 3 turns of HPT¹¹ whilst the Al-3Mg alloy only reaches a uniform microhardness distribution after processing for 10 turns and with an average Vickers microhardness ~180 Hv¹². Additionally, the grains sizes in these materials after 10 turns of HPT are ~230 and ~180-190 nm for the Al-1Mg and the Al-3Mg alloy, respectively. The current investigation demonstrates that the Al-3Mg-0.2Sc alloy continues having an inhomogeneous microhardness distribution even after 10 turns of HPT processing and further grain refinement is achieved by comparison with these Al-Mg alloys.

Similarly to the Al-3Mg-0.2Sc alloy processed by HPT, grain coarsening was also reported in Al-Mg alloys after annealing for times varying from 10 min¹¹ to 1 h^{12,35}. Nevertheless, the grain sizes obtained after heat treatment are considerably larger for the Al-3Mg alloy such that HAGBs structures with an average grain size higher than ~30 μm are identified in the HPT-processed material^{12,35}. Furthermore, the Vickers microhardness in the Al-3Mg alloy processed through 10 turns of HPT is ~50 Hv after subsequent annealing at 673 K for 1 h¹² which is inferior to the average hardness of the HPT-processed Al-3Mg-0.2Sc alloy annealed at equivalent conditions (~78 Hv).

The grain boundary strengthening at low deformation temperatures may be expressed in terms of the Hall-Petch relationship considering the Vickers microhardness, H, and the average grain size, d, as follows³⁶:

$$H = H_0 + k_H d^{1/2} \quad (1)$$

where H_0 and k_H are material constants.

There have been numerous exploratory studies discussing the validity of the Hall-Petch relationship for Al-Mg and Al-Mg-Sc alloys processed by ECAP and HPT^{12,18,22,26,35,36}. In order to verify if this relationship remains accurate for Al-Mg-Sc alloys, the Vickers

microhardness is plotted as a function of $d^{-1/2}$ for the Al-3Mg^{12,35} and the Al-3Mg-0.2Sc alloy after HPT processing at ambient temperature and after HPT followed by annealing for 1 h at temperatures ranging from 423 to 773 K, as depicted in Figure 5.

It is noted from Figure 5 that there is a linear relationship between H and $d^{-1/2}$ for the Al-3Mg-0.2Sc alloy processed by HPT at room temperature regardless of the annealing conditions. In addition, both the experimental datum points referring to the Al-3Mg-0.2Sc alloy and the data plotted for the HPT-processed Al-3Mg alloy corresponding to $d^{-1/2} < \sim 2500$ m^{-1/2} lie close to a single line with $H_0 = 31$ Hv and $k_H \approx 0.06$ Hv m^{-1/2}.

Figure 5 also reveals an apparent breakdown in the Hall-Petch relationship in the Al-3Mg alloy for $d < \sim 0.25$ μm whereas the Hall-Petch relationship remains valid for the Al-3Mg-0.2Sc alloy in the entire range of grain sizes evaluated in this and other studies²². The apparent absence of saturation in the hardness values of the Al-3Mg-0.2Sc alloy after 10 turns of HPT as well as the continuing linearity between H and $d^{-1/2}$ indicate that the UFG metal with Sc additions deforms primarily by intragranular dislocation glide at ambient temperature. There is experimental evidence of deformation-induced segregation of Mg at grain boundaries and triple junctions in Al-Mg-Sc alloys during SPD processing^{22,26}. Therefore, as these segregations are effective on suppressing the emission of extrinsic dislocations, they permit the action of intragranular slip as the most favourable deformation mechanism in this Al alloy at low homologous temperatures. Nevertheless, it is important to note that Mg segregation is not observed in the Al-3Mg alloy after high-pressure torsion which underwent instead dissolution of Mg atoms in solid solution during processing¹².

Severe plastic deformation through HPT processing leads to further strain hardening and grain refinement in the Al-3Mg-0.2Sc alloy²³⁻²⁷ compared with the same alloy processed by ECAP¹⁹⁻²². By contrast, the present work demonstrates that the material processed by HPT displays a more significant grain growth after post-SPD annealing by comparison with

different Al-Mg-Sc alloys processed by ECAP and annealed at $T > 623 \text{ K}^{15,18}$. The reasons for this apparent dichotomy may be assessed by considering the stored strain energy in the work-pieces after SPD processing. Even considering the temperature rise of the Al-3Mg-0.2Sc sample during HPT processing estimated as $\sim 30 \text{ K}$ using an empirical relationship^{37,38}, the density of microstructural defects in the material processed through 10 turns of HPT processing is notable higher than in the Al alloy processed by ECAP. Therefore, as the strain energy stored in the form of internal defects provides the driving force for recrystallization, this phenomenon starts at lower annealing temperatures in the HPT-processed alloy.

A maximum elongation of $\sim 800 \%$ was reported for the Al-3Mg-0.2Sc alloy processed by 10 turns of HPT and tested in tension at $1.4 \times 10^{-2} \text{ s}^{-1}$ at 573 K^{28} . Conversely, the elongations attained in this material after testing at an identical strain rate at $T \geq 623 \text{ K}$ are $< 470 \%$. These results are consistent with the grain size distributions presented in this study. Although, the Al-3Mg-0.2Sc alloy processed through 10 turns of HPT exhibits a duplex microstructure with grain sizes exceeding $10 \mu\text{m}$ after annealing at 623 K , the grain structures in this alloy remain ultrafine and homogeneously distributed after annealing at $T \leq 573 \text{ K}$. It is therefore concluded that the HPT-processed Al-3Mg-0.2Sc alloy is a potential candidate for applications demanding light-weight materials fabricated through superplastic forming at low temperatures.

5. Summary and conclusions

1. An Al-3% Mg-0.2% Sc alloy was processed through 10 turns of HPT at room temperature to produce a grain size of $\sim 140 \text{ nm}$ and an average microhardness of $\sim 190 \text{ Hv}$. Afterwards, annealing was conducted for 1 h at temperatures ranging from 423 to 773 K .

2. There is no significant change in the microstructure of the HPT-processed metal after annealing at 423 K . Nevertheless, there is a substantial reduction in the hardness values and a sharp increase in the grain sizes after annealing at $T \geq 473 \text{ K}$, although the grains remain ultrafine and have a reasonably uniform distribution after annealing at 573 K .

3. Recrystallization occurs inhomogeneously leading to an abnormal grain growth and to a bi-modal distribution of grains after annealing at $T \geq 623$ K, and this becomes more uniform with increasing temperatures.

Acknowledgements

This work was supported by FAPEMIG under Collaborative Grant No. 515139108 between the University of Southampton and the Universidade Federal de Minas Gerais, by CAPES in Brazil and by the European Research Council under ERC Grant Agreement No. 267464-SPDMETALS.

References

- [1] Filatov YuA, Yelagin VI, Zakharov VV. New Al-Mg-Sc alloys. *Materials Science and Engineering: A*. 2000;280:97-101.
- [2] Miller WS, Zhuang L, Bottema J, Wittebrood AJ, De Smet P, Haszler A, Vieregge A. Recent development in aluminium alloys for the automotive industry. *Materials Science and Engineering: A*. 2000;280:37-49.
- [3] Valiev RZ, Islamgaliev RK, Alexandrov IV. Bulk nanostructured materials from severe plastic deformation. *Progress in Materials Science*. 2000;45:103-189.
- [4] Langdon TG. Twenty-five years of ultrafine-grained materials: Achieving exceptional properties through grain refinement. *Acta Materialia*. 2013;61:7035-7059.
- [5] Sabirov I, Murashkin MYu, Valiev RZ. Nanostructured aluminium alloys produced by severe plastic deformation: New horizons in development. *Materials Science and Engineering: A*. 2013;560:1-24.
- [6] Valiev RZ, Langdon TG. Principles of equal-channel angular pressing as a processing tool for grain refinement. *Progress in Materials Science*. 2006;51:881-981.
- [7] Zhilyaev AP, Langdon TG. Using high-pressure torsion for metal processing: Fundamentals and applications. *Progress in Materials Science*. 2008;53:893-979.
- [8] Iwahashi Y, Horita Z, Nemoto M, Langdon TG. Factors influencing the equilibrium grain size in equal-channel angular pressing: Role of Mg additions to aluminum. *Metallurgical and Materials Transactions A*. 1998;29:2503-2510.
- [9] Gubicza J, Chinh NQ, Horita Z, Langdon TG. Effect of Mg addition on microstructure and mechanical properties of aluminium. *Materials Science and Engineering: A*. 2004;387-389:55-59.
- [10] Chen YJ, Chai YC, Roven HJ, Gireesh SS, Yu YD, Hjelen J. Microstructure and mechanical properties of Al-xMg alloys processed by room temperature ECAP. *Materials Science and Engineering: A*. 2012;545:139-147.

- [11] Andreau O, Gubicza J, Zhang NX, Huang Y, Jenei P, Langdon TG. Effect of short-term annealing on the microstructures and flow properties of an Al-1% Mg alloy processed by high-pressure torsion. *Materials Science and Engineering: A*. 2014;615:231-239.
- [12] Lee HJ, Han JK, Janakiraman S, Ahn B, Kawasaki M, Langdon TG. Significance of grain refinement on microstructure and mechanical properties of an Al-3% Mg alloy processed by high-pressure torsion. *Journal of Alloys and Compounds*. 2016;686:998-1007.
- [13] Wang J, Iwahashi Y, Horita Z, Furukawa M, Nemoto M, Valiev RZ, Langdon TG. An investigation of microstructural stability in an Al-Mg alloy with submicrometer grain size. *Acta Materialia*. 1996;44:2973-2982.
- [14] Morris DG, Muñoz-Morris MA. Microstructure of severely deformed Al-3Mg and its evolution during annealing. *Acta Materialia*. 2002;50:4047-4060.
- [15] Lee S, Utsunomiya A, Akamatsu H, Neishi K, Furukawa M, Horita Z, Langdon TG. Influence of scandium and zirconium on grain stability and superplastic ductilities in ultrafine-grained Al-Mg alloys. *Acta Materialia*. 2002;50:553-564.
- [16] Røyset J, Ryum N. Scandium in aluminium alloys. *International Materials Reviews*. 2005;50:19-44.
- [17] Dám K, Lejček P, Michalcová A. In situ TEM investigation of microstructural behavior of superplastic Al-Mg-Sc alloy. *Materials Characterization*. 2013;76:69-75.
- [18] Avtokratova E, Sitdikov O, Mukhametdinova O, Markushev M, Narayana Murty SVS, Prasad MJNV, Kashyap BP. Microstructural evolution in Al-Mg-Sc-Zr alloy during severe plastic deformation and annealing. *Journal of Alloys and Compounds*. 2016;673:182-194.
- [19] Komura S, Horita Z, Furukawa M, Nemoto M, Langdon TG. An evaluation of the flow behavior during high strain rate superplasticity in an Al-Mg-Sc alloy. *Metallurgical and Materials Transactions A*. 2001;32:707-716.

- [20] Avtokratova E, Sitdikov O, Markushev M, Mulyukov R. Extraordinary high-strain rate superplasticity of severely deformed Al-Mg-Sc-Zr alloy. *Materials Science and Engineering: A*. 2012;538:386-390.
- [21] Zhemchuzhnikova D, Kaibyshev R. Mechanical behavior of an Al-Mg-Mn-Sc alloy with an ultrafine grain structure at cryogenic temperatures. *Advanced Engineering Materials*. 2015;17:1804-1811.
- [22] Pereira PHR, Wang YC, Huang Y, Langdon TG. Influence of grain size on the flow properties of an Al-Mg-Sc alloy over seven orders of magnitude of strain rate. *Materials Science and Engineering: A*. 2017;685:367-376.
- [23] Sakai G, Horita Z, Langdon TG. Grain refinement and superplasticity in an aluminum alloy processed by high-pressure torsion. *Materials Science and Engineering: A*. 2005;393:344-351.
- [24] Perevezentsev VN, Shcherban MY, Murashkin MY, Valiev RZ. High-strain-rate superplasticity of nanocrystalline aluminum alloy. *Technical Physics Letters*. 2007;33:648-650.
- [25] Horita Z, Langdon TG. Achieving exceptional superplasticity in a bulk aluminum alloy processed by high-pressure torsion. *Scripta Materialia*. 2008;58:1029-1032.
- [26] Valiev RZ, Enikeev NA, Murashkin MY, Kazykhanov VU, Sauvage X. On the origin of the extremely high strength of ultrafine-grained Al alloys produced by severe plastic deformation. *Scripta Materialia*. 2010;63:949-952.
- [27] Pereira PHR, Huang Y, Langdon TG. Influence of initial heat treatment on the microhardness evolution of an Al-Mg-Sc alloy processed by high-pressure torsion. *Materials Science Forum*. 2017;879:1471-1476.
- [28] Pereira PHR, Huang Y, Langdon TG. Examining the mechanical properties and superplastic behaviour in an Al-Mg-Sc alloy after processing by HPT. *Letters on Materials*. 2015;5:294-300.

- [29] Figueiredo RB, Cetlin PR, Langdon TG. Using finite element modeling to examine the flow processes in quasi-constrained high-pressure torsion. *Materials Science and Engineering: A*. 2011;528:8198-8204.
- [30] Pereira PHR, Figueiredo RB, Cetlin PR, Langdon TG. Using finite element modeling to examine the flow process and temperature evolution in HPT under different constraining conditions. *IOP Conference Series: Materials Science and Engineering*. 2014;63:012041.
- [31] Pereira PHR, Figueiredo RB, Cetlin PR, Langdon TG. An examination of the elastic distortions of anvils in high-pressure torsion. *Materials Science and Engineering: A*. 2015;631:201-208.
- [32] Kawasaki M, Langdon TG. The significance of strain reversals during processing by high-pressure torsion. *Materials Science and Engineering: A*. 2008;498:341-348.
- [33] Røyset J, Ryum N. Kinetics and mechanisms of precipitation in an Al-0.2 wt.% Sc alloy. *Materials Science and Engineering: A*. 2005;396:409-422.
- [34] Ghosh P, Renk O, Pippan R. Microtexture analysis of restoration mechanisms during high pressure torsion of pure nickel. *Materials Science and Engineering: A*. 2017;684:101-109.
- [35] Furukawa M, Horita Z, Nemoto M, Valiev RZ, Langdon TG. Microhardness measurements and the Hall-Petch relationship in an Al-Mg alloy with submicrometre grain size. *Acta Materialia*. 1996;44:4619-4629.
- [36] Furukawa M, Horita Z, Nemoto M, Valiev RZ, Langdon TG. Factors influencing the flow and hardness of materials with ultrafine grain sizes. *Philosophical Magazine A*. 1998;78:203-206.
- [37] Figueiredo RB, Pereira PHR, Aguilar MTP, Cetlin PR, Langdon TG. Using finite element modeling to examine the temperature distribution in quasi-constrained high-pressure torsion. *Acta Materialia*. 2012;60:3190-3198.

- [38] Pereira PHR, Figueiredo RB, Huang Y, Cetlin PR, Langdon TG. Modeling the temperature rise in high-pressure torsion. *Materials Science and Engineering: A*. 2014;593:185-188.

Figure captions:

Figure 1. Variation of the average microhardness recorded at the middle-section position with distance from the centre of the Al-3Mg-0.2Sc discs after HPT processing at 300 K and further annealing.

Figure 2. Average microhardness as a function of annealing temperature for the Al-3Mg-0.2Sc alloy subjected to 10 turns of HPT processing at 300 K and further annealed for 1 h at temperatures from 423 to 773 K.

Figure 3. Grain size as a function of annealing temperature for the Al-3Mg-0.2Sc alloy subjected to 10 turns of HPT processing at 300 K and further annealed for 1 h at temperatures from 423 to 773 K.

Figure 4. Grain size coloured images of the grain structures of the Al-3Mg-0.2Sc alloy processed by HPT at 300 K and further annealed for 1 h at (a) 573, (b) 623 and (c) 773 K.

Figure 5. Plot of Vickers microhardness as a function of $d^{-1/2}$ for the Al-3Mg^{12,35} and the Al-3Mg-0.2Sc alloy after HPT processing at ambient temperature and after HPT followed by annealing for 1 h at temperatures ranging from 423 to 773 K.

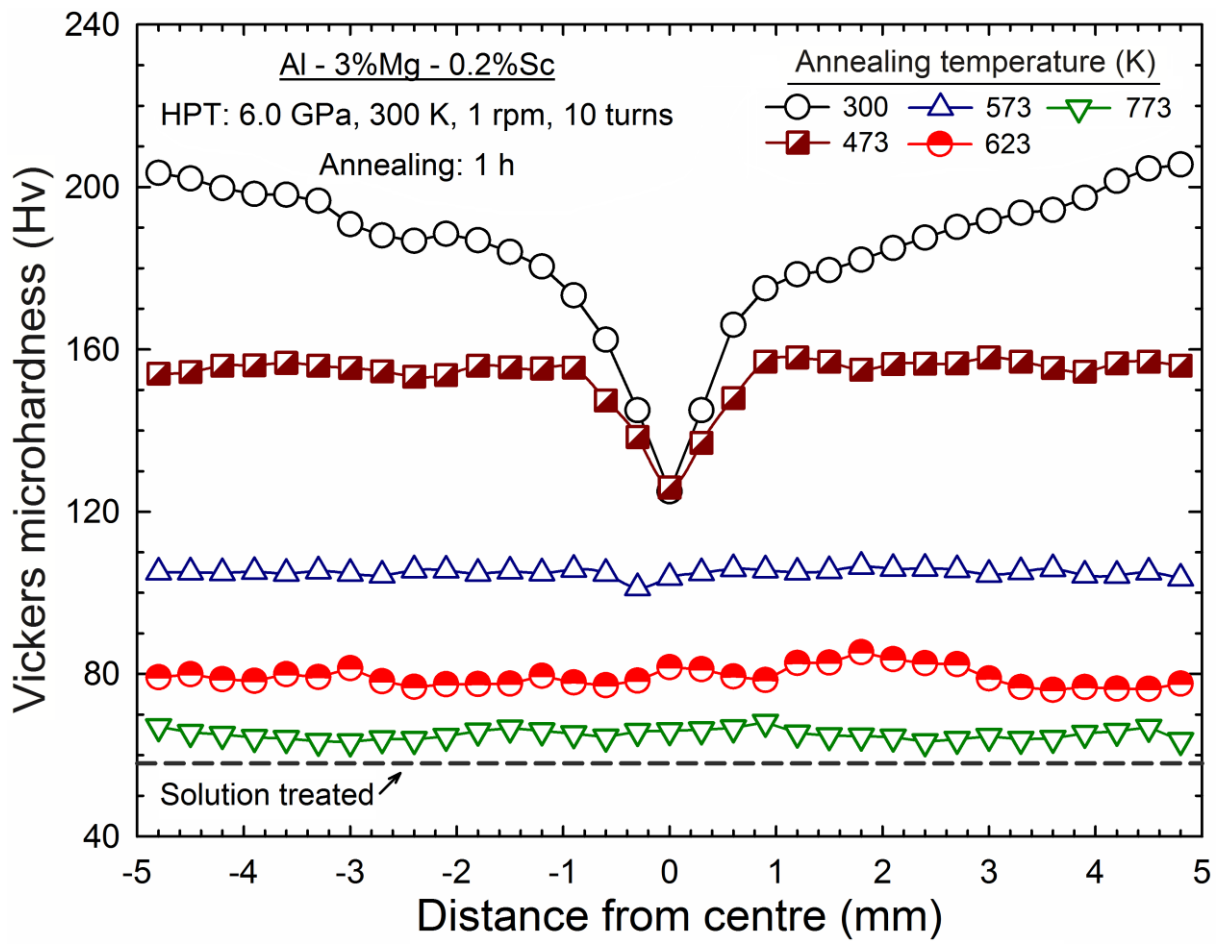


Figure 1

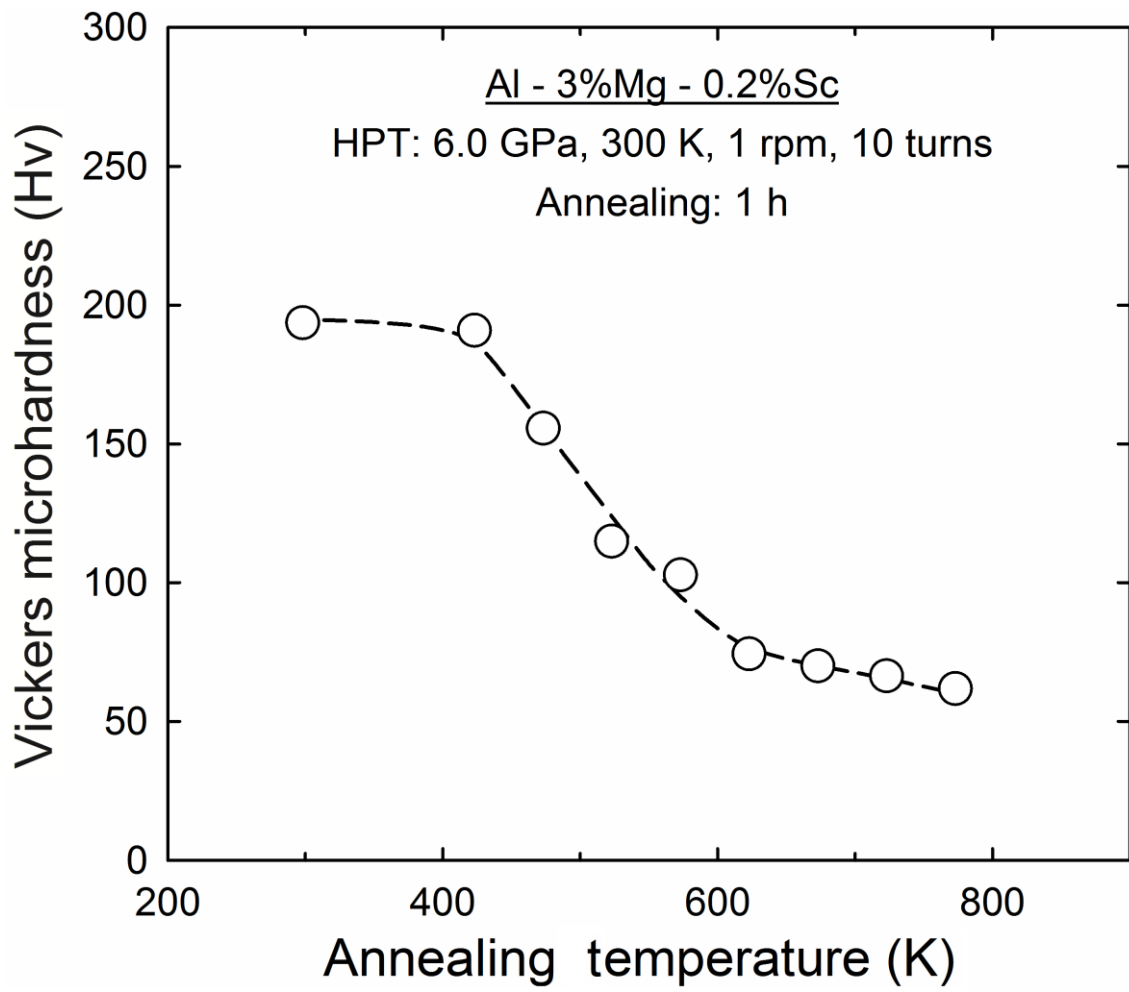


Figure 2

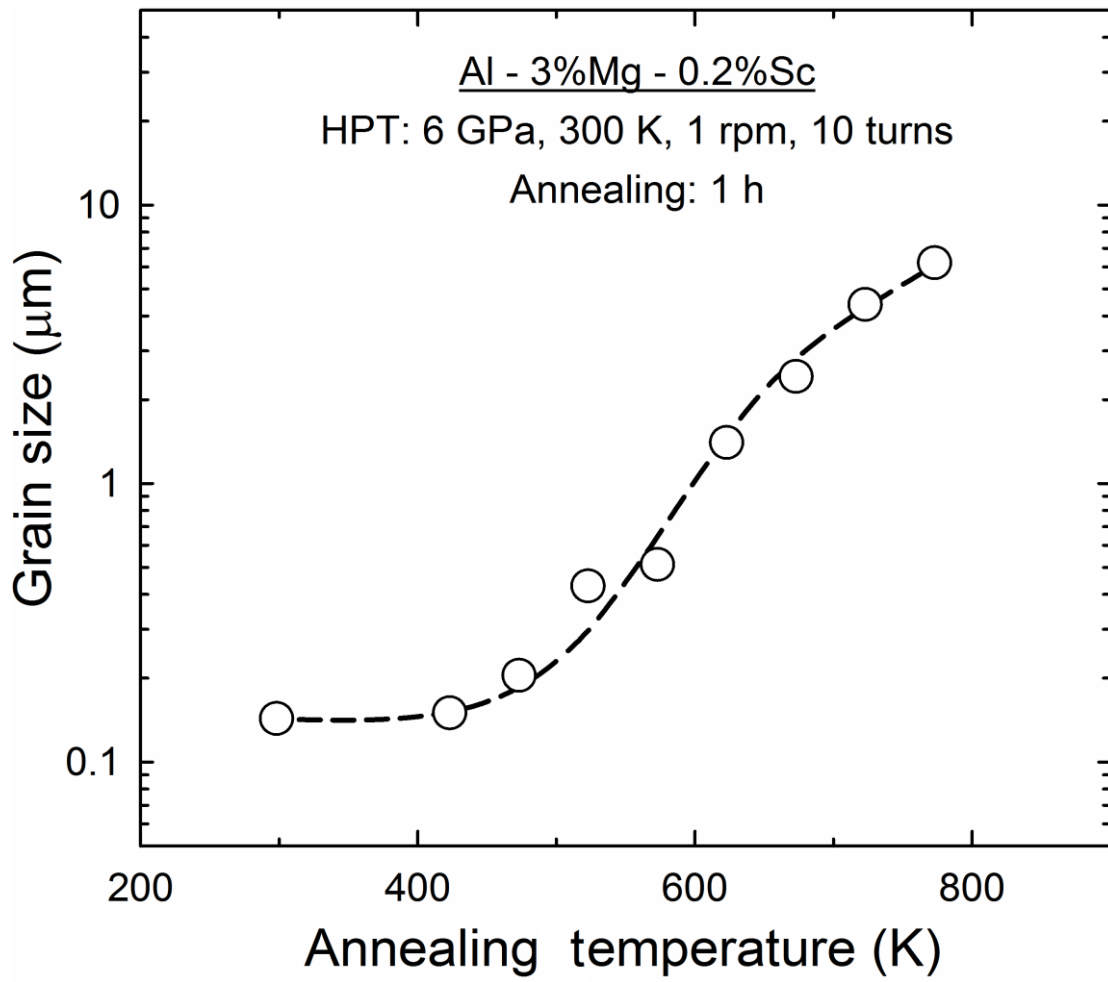
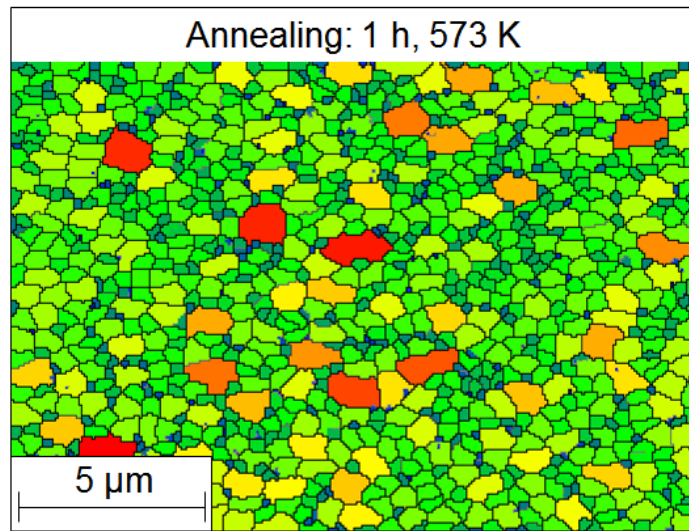


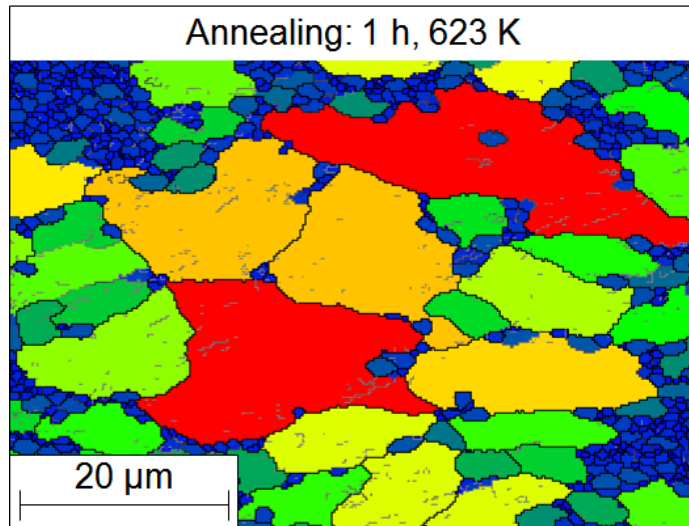
Figure 3

Al – 3%Mg – 0.2%Sc
HPT: 6 GPa, 10 turns, 300 K, 1 rpm

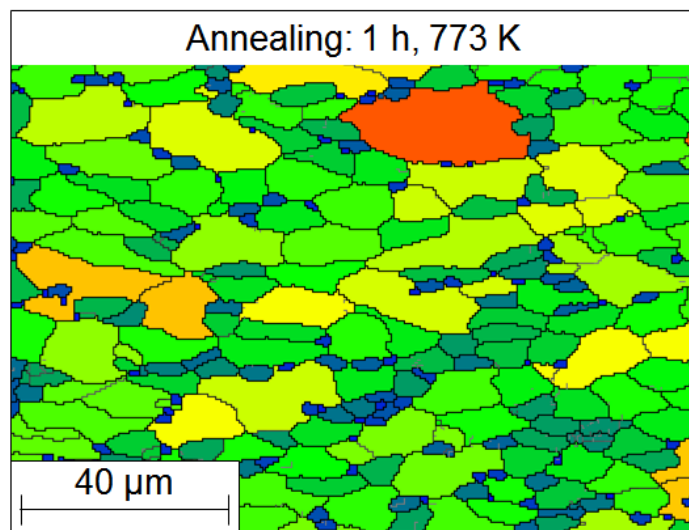
— 2 - 15°
— > 15°



(a)



(b)



(c)

Figure 4

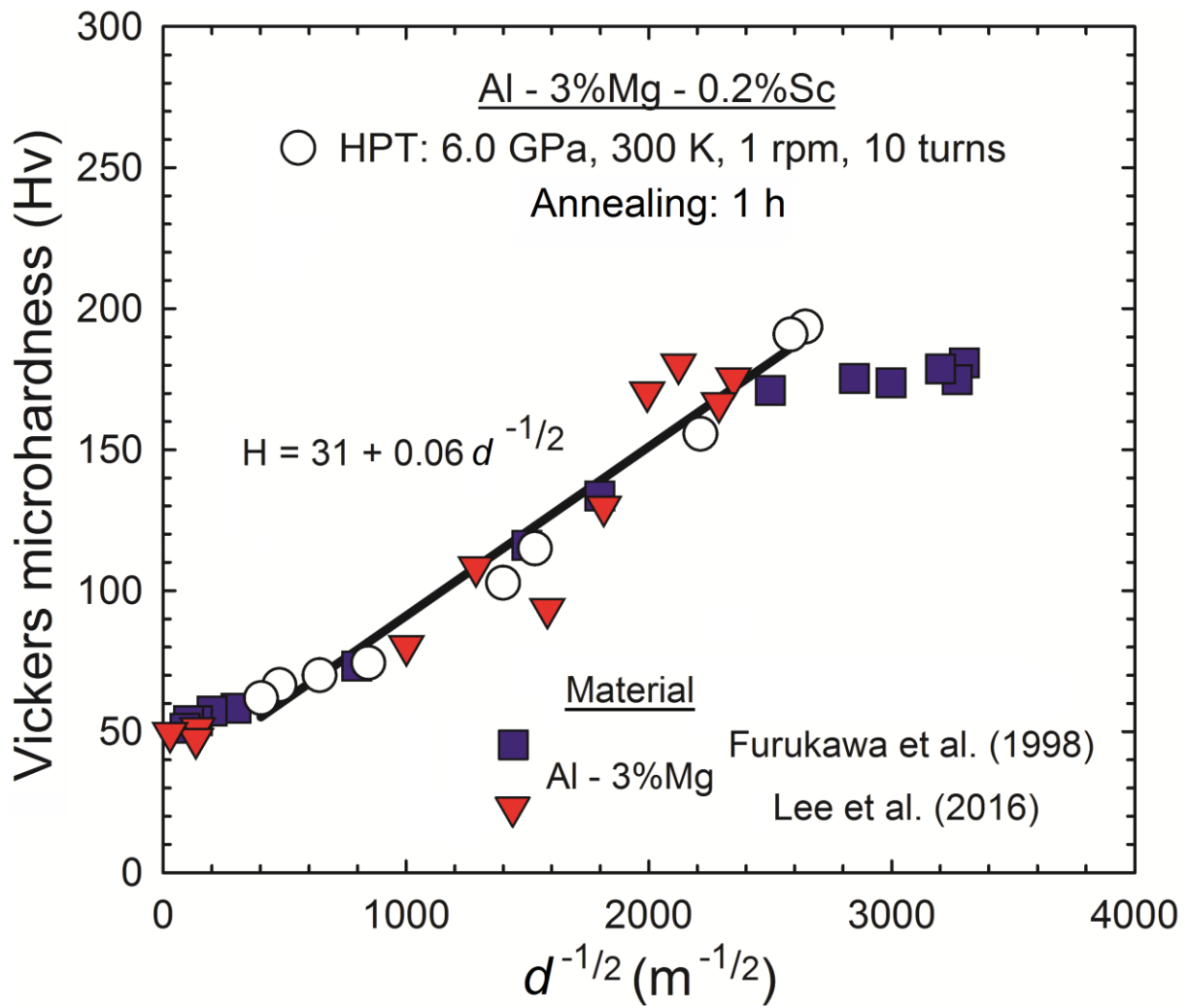


Figure 5